ERDC/EL TR-05-10

US Army Corps
of Engineers®
Engineer Research and
Development Center

Environmental Quality Technology (EQT) Program

Electrolytic Transformation of Hexahydro-1,3,5-Trinitro-1,3,5-Triazine (RDX) and 2,4,6-Trinitrotoluene (TNT) in Aqueous Solutions

Altaf H. Wani, Brenda R. O'Neal, David M. Gilbert,
David B. Gent, and Jeffrey L. Davis

August 2005

Environmental Laboratory

Environmental Quality Technology (EQT) Program

ERDC/EL TR-05-10
August 2005

Electrolytic Transformation of Hexahydro-1,3,5-Trinitro-1,3,5-Triazine (RDX) and 2,4,6-Trinitrotoluene (TNT) in Aqueous Solutions

Altaf H. Wani

Applied Research Associates, Inc.
Southern Division
119 Monument Place
Vicksburg, MS 39180-6199

Brenda R. O'Neal

Analytical Services, Inc.
3532 Manor Drive
Vicksburg, MS 39180-6199

David M. Gilbert

Department of Civil Engineering
Colorado State University
Fort Collins, CO 80523

David B. Gent, Jeffrey L. Davis

Environmental Laboratory
U.S. Army Engineer Research and Development Center
3909 Halls Ferry Road
Vicksburg, MS 39180-6199

Final report

Prepared for U.S. Army Corps of Engineers
Washington, DC 20314-1000

Under EQT Work Unit D03E

ABSTRACT: Electrolytic reactive barriers (e^-barriers) consist of closely spaced permeable electrodes installed across a groundwater contaminant plume in a permeable reactive barrier format. Application of sufficient potential to the electrodes results in sequential oxidation and reduction of the target contaminant. The objective of this study was to quantify the mass distribution of compounds produced during sequential electrolytic oxidation and reduction of ordinance related compounds (ORCs) in a laboratory analog to an e^-barrier. In this study, a series of column tests were conducted using RDX (hexahydro-1,3,5-trinitro-1,3,5-triazine) and TNT (2,4,6-trinitrotoluene) as representative ORCs. The experimental setup consisted of a Plexiglass column packed with quart-feldspar sand to simulate aquifer conditions. A single set of porous electrodes consisting of expanded titanium-mixed metal oxide mesh was placed at the midpoint of the soil column as a one-dimensional analog to an e^-barrier. Constant current of 20 mA (variable voltage) was applied to the electrode set. Initial studies involved quantification of reaction products using unlabeled RDX and TNT. Approximately 70 percent of the influent concentration was transformed, in one pass, through sequential oxidation-reduction for both contaminants. Following the unlabeled studies, ^{14}C labeled RDX and TNT were introduced to determine the mass balance. An activity balance of up to 96 percent was achieved for both ^{14}C-RDX and ^{14}C-TNT. For both contaminants, approximately 21 percent of the influent activity was mineralized to $^{14}CO_2$. The proportion of the initial activity in the dissolved fraction was different for the two test contaminants. Approximately 30 percent of the initial ^{14}C-RDX was recovered as unreacted in the dissolved phase. The balance of the ^{14}C-RDX was recovered as non-volatile, non-nitroso transformation products. None of the ^{14}C-RDX was sorbed to the column sand packing. For ^{14}C-TNT approximately 51 percent of the initial activity was recovered in the dissolved phase, the majority being unreacted TNT. The balance of the ^{14}C-TNT was either sorbed to the sand packing (approximately 24 percent) or dissolved/mineralized as unidentified ring cleavage products (~4 percent).

Contents

Preface v

1—Introduction 1

2—Materials and Methods 4

Electrolytic Reactive Barrier 4
Reagents and Operation 5
Analytical Techniques 7

3—Results and Discussion 9

RDX Transformation 9
RDX Radiocarbon (^{14}C) Distribution 11
TNT Transformation 13
TNT Radiocarbon (^{14}C) Distribution 14

4—Conclusions 17

References 18

Appendix A: Column Hydrodynamics 1

SF 298

List of Figures

Figure 1. Schematics of an e^- barrier system 1

Figure 2. Schematics of water electrolysis under DC electrical field 2

Figure 3. Experimental setup: (a) cold study, (b) radiolabel study 5

Figure 4. Sampling and analysis schematic used for the radiocarbon study 6

Figure 5. Chloride tracer breakthrough curve 9

Figure 6. Operating current and voltage as a function of time for RDX test: (a) current and cell potential and (b) electrode potentials relative to Ag/AgCl reference half-cells 10

Figure 7. RDX concentration, in the influent and effluent to the column, as a function of time 11

Figure 8. RDX concentration as a function of distance from the column inlet. 12

Figure 9. Distribution of ^{14}C activity from ^{14}C-RDX 12

Figure 10. Operating current and voltage as a function of time for TNT test: (a) current and cell potential and (b) electrode potentials relative to Ag/AgCl reference half-cells 13

Figure 11. TNT concentration in e^-barrier column influent and effluent stream 14

Figure 12. Axial TNT concentration profile along column length 15

Figure 13. Distribution of ^{14}C activity from ^{14}C-TNT 16

Preface

The purpose of this research project was to develop an in situ electrolytic remediation technology for ORC contaminated groundwater and to evaluate the mass balance of RDX and TNT electrolytic transformation in groundwater using radiolabeled RDX and TNT. A series of column studies were conducted using quartz-feldspar sand to simulate the aquifer material.

The research was conducted at the Environmental Laboratory (EL), U.S. Army Engineer Research and Development Center (ERDC), Vicksburg, MS. The funding for this project was provided by the Environmental Quality Technology Program under project AF-25.

This report was prepared by Dr. Altaf H. Wani, Applied Research Associates, Inc., Vicksburg, MS; Ms. Brenda R. O'Neal, Analytical Services, Inc., Vicksburg, MS; Dr. David M. Gilbert, Department of Civil Engineering, Colorado State University, Fort Collins, CO; and Mr. David B. Gent and Dr. Jeffrey L. Davis, Environmental Engineering Branch (EEB), EL.

Authors gratefully acknowledge the financial support provided by the U.S. Army's Research, Development, Technology, and Evaluation (RDTE) Program. The findings and conclusions reported in this publication are exclusively those of the authors and do not necessarily reflect the views of U.S. Army.

This study was conducted under the direct supervision of Dr. Patrick N. Delimen, Chief, EEB, and Dr. Richard E. Price, Chief, Environmental Processes and Engineering Division, EL, and under the general supervision of Dr. Edwin A. Theriot, Director, EL.

COL James R. Rowan, EN, was Commander and Executive Director of ERDC. Dr. James R. Houston was Director.

1 Introduction

Past practices at many explosives manufacturing and storage facilities have resulted in soil and groundwater contamination involving ordinance related compounds (ORCs) such as nitroaromatic and nitramine compounds. Engineered solutions to remediate these sites have focused on groundwater extraction and treatment or in situ manipulation of redox conditions. Unfortunately, many of the available technologies are limited by efficacy and/or cost. Development of low-cost, low maintenance alternatives is needed since many of the contaminated sites are no longer in use. To meet this need, our research has focused on development of electrolytic approaches to transformation of dissolved ORCs. One application is the electrolytic permeable reactive barrier (e^-barrier). The e^-barrier consists of a pair (or multiple pairs) of closely spaced permeable electrodes placed across a groundwater contaminant plume in a permeable reactive barrier (PRB) format. Application of low voltage direct current to the electrodes drives sequential oxidation and reduction at the anode and cathode respectively (Figure 1).

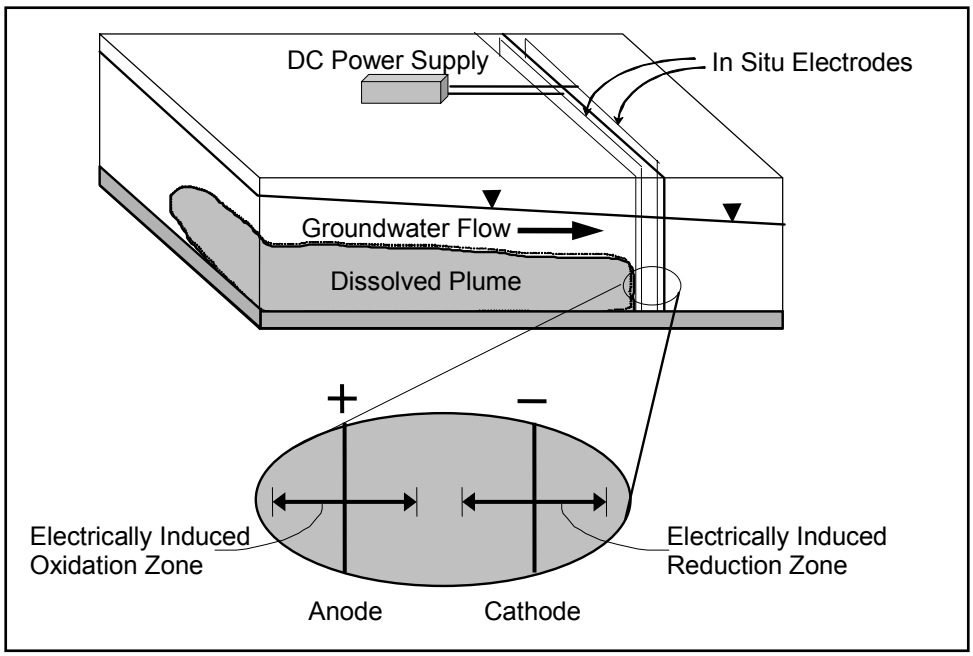

Figure 1. Schematics of an e^-barrier system

It is well known that application of DC electric current through electrodes immersed in water induces electrolysis reactions at the electrodes. Oxidation of water produces oxygen gas and an acid (H^+) front at the anode, while water reduction results in the production of H_2 gas and a base (OH^-) front at the cathode, as illustrated in Figure 2. Based on Faraday's law for equivalence of mass and charge, the rate of electrolysis reactions depends on the total current applied. For water oxidation at the anode, the rate of electrolysis is given by:

$$J = \frac{I}{z \cdot F} \tag{1}$$

where

J = rate of oxidation or reduction by electrolysis (M/T)

I = current (A)

z = charge of the ion (for hydrogen $z = 1$)

F = Faraday's constant (96,485 Coulomb/mole)

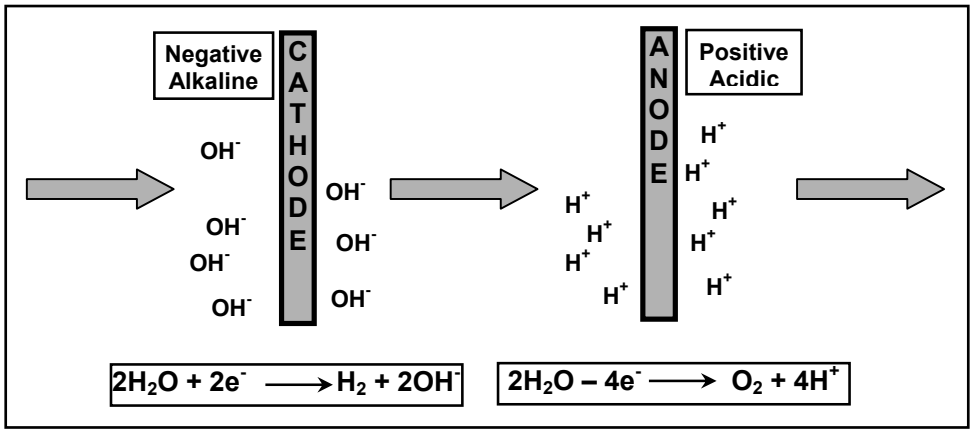

Figure 2. Schematics of water electrolysis under DC electrical field

However, it should be noted that other electrolysis reactions may occur and limit the water electrolysis reaction. The electrolysis reaction depends upon the chemistry of the electrolyte, pH, and the standard electrode potential for ions in the electrolyte. Acar and Alshawabkeh (1993) demonstrated that irrespective of some secondary reactions favored at the cathode because of their lower electrochemical potential, the water reduction half-reaction (H_2O/H_2) is dominant at early stages of the process that causes the pH to drop below 2 at the anode and to raise above 10 at the cathode, depending upon the total current applied. While the acid generated at the anode advances toward the cathode by ionic migration and electro-osmosis, the base developed at the cathode initially advances toward the anode by diffusion and ionic migration. The advance of the base front is slower than the advance of the acid front because of the counteracting electro-osmotic flow and also because the ionic mobility of H^+ is about 1.76 times that of OH^-. As a consequence, the acid front dominates except for sections close to the cathode (Alshawabkeh and Acar 1992; Probstein and Hicks 1993). Furthermore, geochemical reactions in the aquifer material significantly impact the electrolysis

reaction, either enhancing or retarding the process. These are some of the concerns that need to be answered for field-scale validation/demonstration of this cost-effective in situ treatment technology. This research project will evaluate some of these concerns and lay the groundwork for the future efforts.

The e^-barrier provides many potential advantages to existing PRB technologies including:

a. The method is environmentally benign, in that no chemicals are introduced.

b. Electrical power costs associated with driving transformation of energetic compounds are estimated to be low. Based on laboratory and field demonstration tests, power costs associated with operation of an e^-barrier are approximately \$0.013 m^{-2} d^{-1} (Sale et al. 2005).

c. Rates of chemical transformation can be modified remotely by adjusting applied voltage.

d. The electrode potentials can be reversed or shifted to remove inorganic precipitates (e.g., $CaCO_3$ scale, a common constraint of other technologies).

e. Primary components are commercially available off-the-shelf items.

Electrolytic treatment of aqueous organic compounds has received attention for several years (Bunce et al. 1997; de Lima Leite et al. 2003; Panizza and Cerisola 2004). Treatment is achieved by either oxidation (anodic) or reduction (cathodic) of the target contaminant and has been applied to dye wastes (Roessler et al. 2002), landfill leachates (Vlyssides et al. 2003) and other aqueous organic compounds including ORCs (Bonin et al. 2004; Doppalapudi et al. 2003; Jimenez-Jado et al. 2004; Jolas et al. 2000; Maloney et al. 1999; Mills et al. 2003; Rodgers and Bunce 2001).

Electrolytic treatment of ORCs has received increasing attention since coupled oxidative and reductive steps are possible using a single electrochemical cell (Bonin et al. 2004; Gilbert and Sale 2005). Laboratory experiments conducted to date involving sequential electrolytic oxidation and reduction have focused primarily on proof-of-concept and transformation efficacy (Gilbert and Sale 2005) and identification of transformation products (Bonin et al. 2004). The research presented here uses a mass balance approach using radiolabeled TNT and RDX in a laboratory analog to an e^-barrier to advance current knowledge by quantifying the products of sequential electrolytic oxidation and reduction of ORCs.

2 Materials and Methods

The experimental design was to monitor electrolytic transformation of ORCs (using RDX and TNT as representative compounds) by pumping dissolved contaminants through a one-dimensional analog to an e$^-$barrier. The approach was to first verify transformation using unlabeled ^{12}C-RDX and ^{12}C-TNT, followed by introduction of radiolabeled (^{14}C) RDX and TNT to conduct the mass balance.

Electrolytic Reactive Barrier

The experimental setup consisted of a horizontally mounted column (96 cm × 10 cm ID) containing a single set of electrodes. The electrode materials (Elgard^{TM} 85 mesh) were coated with a metal oxide catalyst sintered to expanded titanium mesh (Eltech Systems, Chardon, OH). The electrodes were mounted at 38 (anode) and 40 cm (cathode) from the inlet to the e$^-$barrier column. The 2 cm electrode spacing was designed to lower the power requirements, simplify potential field installations, and to maintain pH near neutrality. In this configuration, the treatment sequence was oxidation, followed by reduction. The inter-electrode space was filled with 6 mm glass beads to maintain a 2-cm electrode spacing. The remainder of the e$^-$barrier column was packed with quartz-feldspar sand intended to simulate an aquifer material. The e$^-$barrier column was fitted with Ag/AgCl reference half-cells (World Precision Instruments, Sarasota, FL) installed in the immediate vicinity of the electrodes to measure electrode potentials. Eight glass sample ports spaced along the length of the column allowed for collection of aqueous samples for bed profile analysis (Figure 3a). Test solutions were pumped through the e$^-$barrier column by using a variable speed control Masterflex peristaltic pump. The oxidation-reduction potential (ORP) electrodes were installed at the column inlet and outlet via flow-through cells to compare the redox condition of the effluent with that of the inlet reservoir. During the radiolabel test, the effluent stream from the e$^-$barrier column was collected in a glass sampler under an acid quenching solution to release any dissolved carbon dioxide. The off gases from the acid quencher were passed through carbon dioxide scrubbers (Carbo-Sorb) to absorb carbon dioxide from the gas stream. Gases from the electrode gas vents, during the radiolabel test, were collected in Tedlar bags and extracted using Carbo-Sorb carbon dioxide sorbent (Figure 3b).

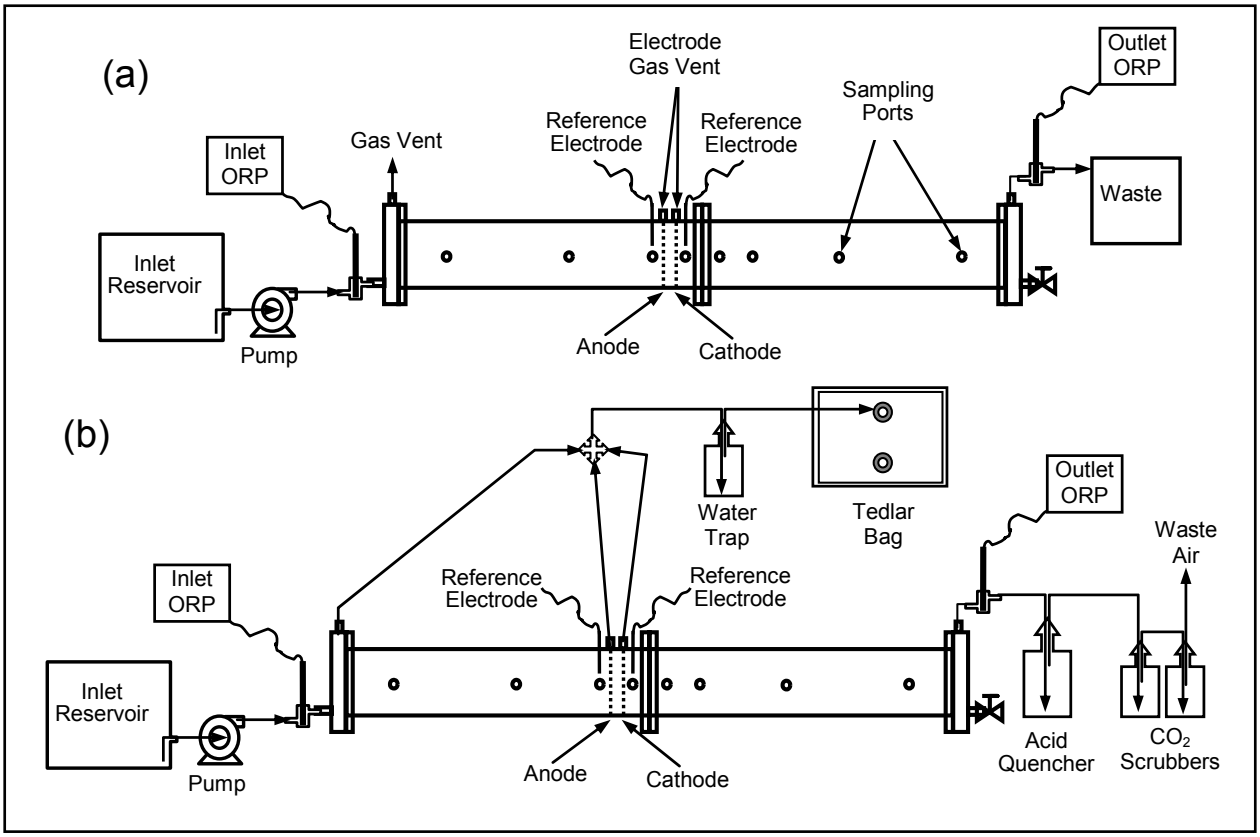

Figure 3. Experimental setup: (a) cold study, (b) radiolabel study

Reagents and Operation

RDX and TNT contaminated water was prepared by spiking aged tap water (415 µS/cm, pH = 7.8) with stock solutions of RDX and TNT. The unlabeled RDX used in the first phase of the study was procured from Holston Ammunition Plant (Kingston, TN), and unlabeled TNT was obtained from Rock Island Arsenal (Rock Island, IL). Radiolabeled ^{14}C-RDX and TNT were obtained from Perkin Elmer Life Sciences (Shelton, CT). RDX and TNT calibration standards for EPA Method 8330 were obtained from Supelco (Boston, MA).

Test waters with individual concentrations of approximately 0.5 mg/L RDX and 0.5 mg/L TNT, respectively, were pumped through the column at a flow of about 0.6 mL/min, equivalent to a seepage velocity of approximately 0.3 m/d. Test solution concentrations were intended to approximate typical RDX and TNT groundwater concentrations observed in the field (~300-600 µg/L). Unlabeled RDX and TNT studies lasted for 60 and 58 days, respectively, before initiating the radiocarbon study. Liquid samples were collected from inlet and outlet sampling ports weekly. After reaching steady state, samples from intermediate ports along the column length were collected for bed profile analysis. Once the column reached equilibrium conditions with steady contaminant removal, a slug of about 160 k Bq (4.32 µCi) ^{14}C-RDX was introduced in the inlet reservoir. For the radiolabeled TNT test, a slug of about 192 k Bq (5.20 µCi) ^{14}C-TNT was used. Effluent liquid stream, including any carbon dioxide evolved as a result of

mineralization, was collected in a 1 L glass sampler under a hydrochloric acid quenching solution (25 mL, 1N HCl) to release any dissolved carbon dioxide. The effluent gases from the acid quencher were passed through carbon dioxide scrubbers containing 100 mL Carbo-Sorb® (Packard Biosciences, CT) to scrub out carbon dioxide from the gas stream. At the end of the sampling, the sampling train (acid quencher-Carbo-Sorb scrubbers) was flushed with nitrogen gas to complete the transfer of all the carbon dioxide from the acid quencher into the Carbo-Sorb scrubbers. The contents of the acid quencher were neutralized with 1N NaOH. Liquid scintillation counting (LSC) was performed on aliquots from the neutralized effluent to estimate the portion of ^{14}C activity in the dissolved phase. A 4 mL aliquot of the neutralized effluent was mixed with 15 mL Ultima Gold® (Packard Biosciences, CT) scintillation cocktail for radioactivity counting (Figure 4). The contents of the Carbo-Sorb scrubbers were subjected to liquid scintillation counting to evaluate the fraction of ^{14}C activity mineralized to ^{14}C-CO_2. A 10 mL aliquot from Carbo-Sorb scrubber was mixed with 10 mL Permafluor® (Packard Biosciences, CT) scintillation cocktail for radioactivity counting. The total radioactivity from the gaseous (mineralization CO_2), the dissolved (nitroso- and non-nitroso-substituted nonvolatile metabolites), and the sorbed phases was summed up and compared with the initial radioactivity introduced as ^{14}C. An aliquot from the neutralized effluent was analyzed for RDX and TNT, as was their transformation metabolites using high performance liquid chromatography (HPLC). Off gases from the electrode gas vents were collected in Tedlar bags and extracted using Carbo-Sorb carbon dioxide sorbent for radiocarbon counting.

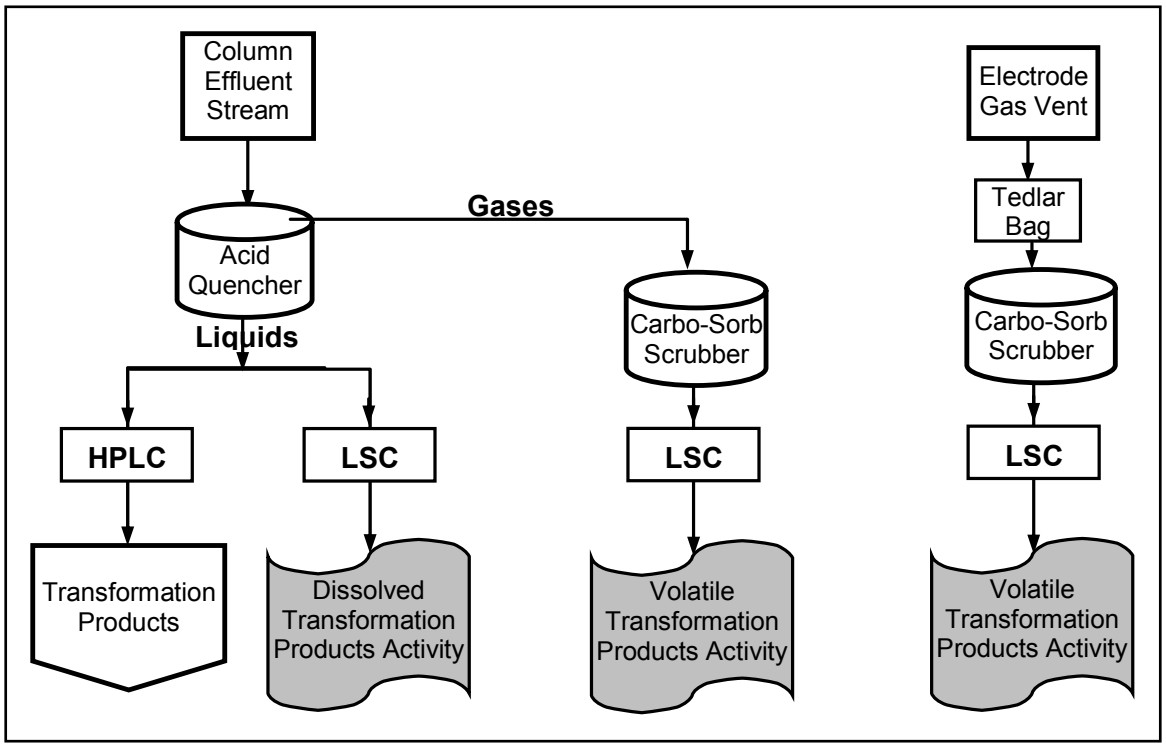

Figure 4. Sampling and analysis schematic used for the radiocarbon study

Analytical Techniques

The primary analysis was to measure the aqueous phase concentrations of RDX, TNT, and known transformation products in the influent and effluent streams. Secondary analysis involved measurement of RDX and TNT concentration as a function of the position along the column. The analysis of RDX, its nitroso-substituted transformation products, and TNT and its daughter products was performed using a DIONEX HPLC system (Sunnyvale, CA) comprised of a P580 fluid pump, ASI-100 autosampler, and UVD340U absorbance detector. The injection volume was 25 µL. Chemical separation for RDX and its nitroso-substituted transformation products was achieved using a Supelco CN reverse-phase HPLC column (250 x 4.6 mm). In case of TNT and its daughter products, Supelco C18 reverse-phase HPLC column (250 x 4.6 mm) was used for chemical separation. For both RDX and TNT and their transformation products, peak absorbance was monitored at 254 nm. The mobile phase comprised of 1:1 (volume per volume) methanol/organic-free reagent water at a flow of 1 mL min^{-1}.

Inorganics (chloride, nitrate, and nitrite) in the liquid samples were analyzed on a DIONEX (Sunnyvale, CA) Ion Chromatograph. Chemical separation and detection were achieved using an Ionpac AS11 analytical column (250 x 4 mm) and a Dionex conductivity detector (1.25 µL internal volume). The mobile phase consisted of NaOH at a flow of 1.5 mL/min. The sample volume was 25 µL of filtered (0.45 µm) sample.

Liquid sample radioactive concentration, via liquid scintillation counting, was conducted on a 2500 TR Packard Scintillation Counter (Packard Biosciences). The counter is equipped with a barium external source to enable correction for machine efficiency. Radioactive carbon sorbed on the sand (column packing) samples was counted by burning the sand samples in a Packard 307 Soil Oxidizer (Packard Biosciences). The burn efficiency of the oxidizer was established at >97 percent. Each sample (~0.2 g) was burned for 75 sec. Every two sand samples were separated by a blank. The samples were counted on a Packard Tri-Carb 2900TR equipped with a barium external source to correct for machine efficiency. The liquid scintillation protocol collected data up to 156 keV (kilo electric volt), which is the maximum spectrum of betas of ^{14}C. Each sample was counted twice for 2 min.

The ORP and pH were measured with Oakton WD-35100-00 model pH/ORP controllers (Cole-Parmer, Vernon Hills, IL), with a measuring range of 0 to 14 for pH and -1250 to 1250 mV ORP. ORP was measured inline via flow-through cells using a Cole-Parmer combination redox electrode with platinum sensing surface and Ag/AgCl reference electrode. The value E_h was obtained by adding the standard potential of the reference electrode (202 mV at 25 °C) to the measured potential. The pH of the liquid samples collected from inlet, outlet, and intermediate sampling ports along the column length was measured using a Cole-Parmer combination electrode.

The single output (DC) power supply (Agilent, Palo Alto, CA), Model E3612A with constant current (CC) and constant voltage (CV) modes, was used in this study. The output voltage and amperage ranged between 0-120V and 0-0.5 A, respectively.

3 Results and Discussion

The quartz-feldspar sand used in this study was predominantly fine sand (16-40, Colorado Silica Sand) with very low total organic content. The results of tracer tests revealed that the e⁻barrier column packing material has an effective porosity of 0.39 and dispersivity of 0.37cm (Figure 5 and Appendix A). The measured porosities were within the values expected for loosely packed sand. The estimated hydraulic conductivity of the sand packing in the e⁻barrier column was 0.12 cm/sec.

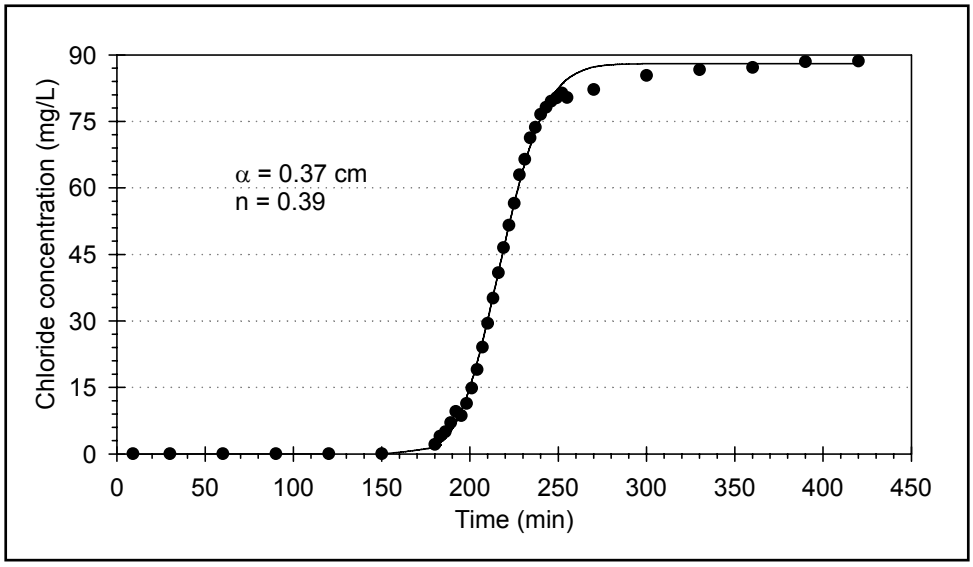

Figure 5. Chloride tracer breakthrough curve

RDX Transformation

Experiments were conducted to evaluate reactor performance using unlabeled RDX-contaminated water prior to initiation of experiments using radiocarbon RDX for assessing the ultimate fate of RDX under sequential electrolytic oxidation and reduction processes. Constant current was applied to the electrodes in two steps, 10 mA for 30 days followed by 30 days at 20 mA (0.05 and 0.10 mA/cm^2, respectively). Applied cell potential increased throughout the first phase of the experiment suggesting a loss in specific conductance, probably as a result of scaling. This behavior was not observed during the second current setting (Figure 6a). Electrode potentials measured against the reference half-cells

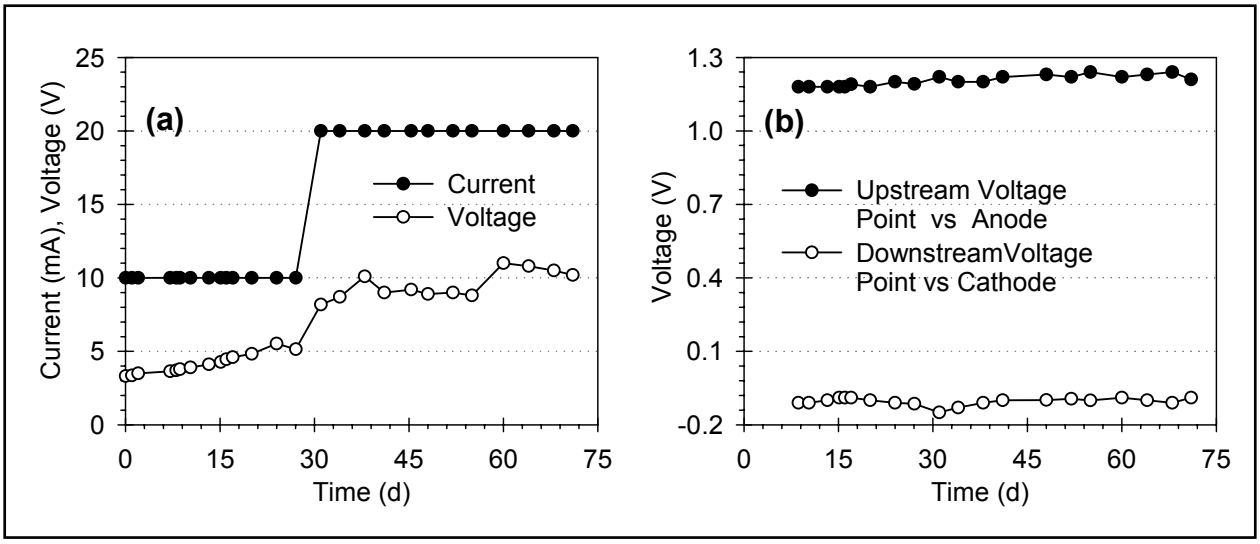

Figure 6. Operating current and voltage as a function of time for RDX test: (a) current and cell potential and (b) electrode potentials relative to Ag/AgCl reference half-cells

positioned near the surface of the electrodes indicated that both anode and cathode potentials remained constant throughout the experiment (Figure 6b). Increase in cell potential from approximately 5 V to 10 V, therefore, did not result in a substantial change in electrode potential, suggesting that surface reactions were resulting in a poisoning of the electrode potential.

RDX concentrations in the influent and effluent streams from the e^-barrier column were monitored over time and suggest that increasing the system current did not result in increased transformation of RDX (Figure 7). This result is consistent with the lack of response of electrode potential with increasing cell potential and current. RDX inlet concentrations of ~0.5 mg/L were reduced to about 0.15 mg/L with very low occasional detections of nitroso-substituted RDX derivatives. Low levels of DNX and TNX were initially observed in the effluent stream as the reductive environment was developing in the column. Reductive conditions were established in the column with the time of operation, and E_h drop between column influent and effluent was between 100 and 150 mV. Aqueous pH levels were relatively constant throughout the column length. The pH remained between 7.5 and 8, thereby eliminating the possibility of alkaline hydrolysis of RDX that occurs at pH 10 and higher (Balakrishnan et al. 2003). During the actual radiolabel test (final 2 weeks of the study), low concentrations of RDX were observed in the effluent stream without the detection of any nitroso metabolites.

The maximum RDX transformed in the e^-barrier was approximately 70 percent. The cumulative presence of RDX and nitroso-substituted RDX metabolites (MNX, DNX, and TNX) in the effluent accounted for about 30 percent of the influent RDX concentration. The unidentified 70 percent of the influent RDX concentration likely includes volatile (including mineralized carbon dioxide) and nonvolatile non-nitroso-transformation products generated as a result of ring cleavage (Halasz et al. 2002; Hawari et al. 2000; McCormick et al. 1981;

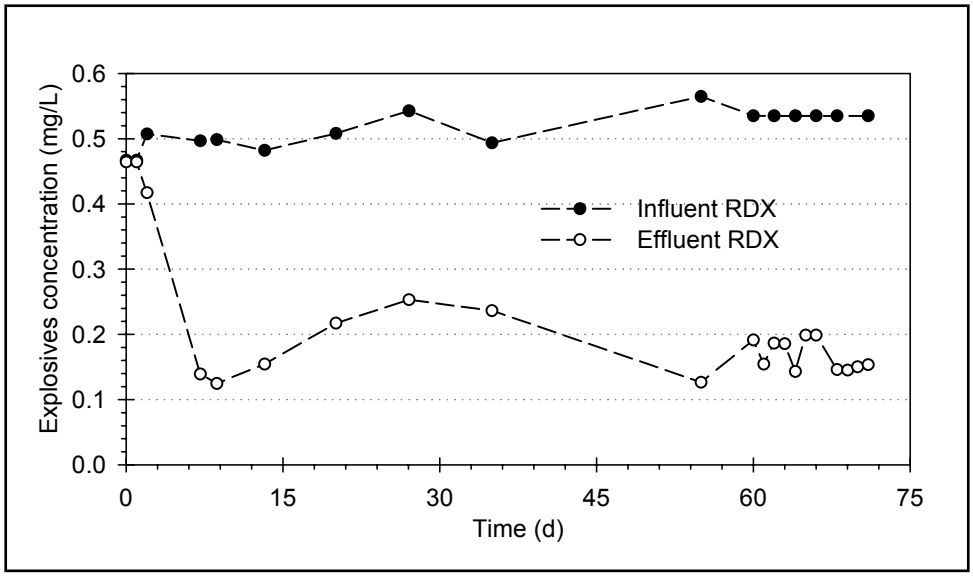

Figure 7. RDX concentration, in the influent and effluent to the column, as a function of time. Arrow indicates the time when slug of radiolabel RDX was introduced

Oh et al. 2001). To close the mass balance, acetonitrile was used to extract RDX or nitroso-substituted derivates from the quartz-feldspar sand. No RDX or nitroso-substituted derivatives were detected.

After reaching steady state, samples from intermediate sampling ports along the column length were collected immediately prior to the radiocarbon study. Concentration profiles taken on day 60 indicated that a majority of the transformation occurred at the electrode surfaces, suggesting that the reactions are the result of heterogeneous electron transfer (Figure 8). Minor (~10 percent) RDX removal was observed upstream of anode, probably due to highly oxidative conditions developed at the anode. The majority of RDX removal was near electrode surfaces. No significant RDX removal was observed downstream of the cathode.

RDX Radiocarbon (^{14}C) Distribution

Once the e^-barrier column reached steady state RDX transformation, a slug (1003.6 mL) of about 160 k Bq (~4.32 µCi) radiolabel RDX was introduced to the column on day 60. After that, 10 bed volumes of unlabeled RDX-contaminated water were pumped through the column over the next 10 days to wash out any radioactivity sorbed on the quartz-feldspar sand packing until the activity in the effluent reached the background level. The distribution of radiocarbon (^{14}C) is summarized in Figure 9. The final activity balance on radiocarbon was more than 92 percent. The radiocarbon activity was distributed into two distinct fractions: (a) dissolved (as aqueous soluble compounds), and (b) mineralized (as carbon dioxide). The activity balance on ^{14}C-RDX indicated that approximately 20 percent of the influent ^{14}C-RDX was transformed to $^{14}CO_2$, as

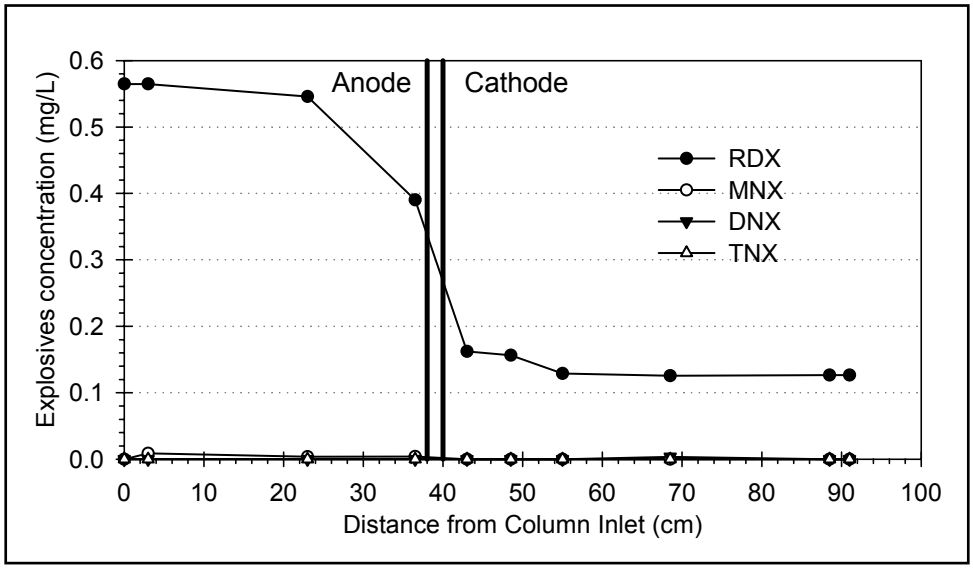

Figure 8. RDX concentration as a function of distance from the column inlet. The electrodes were set at 38 cm (anode) and 40 cm (cathode)

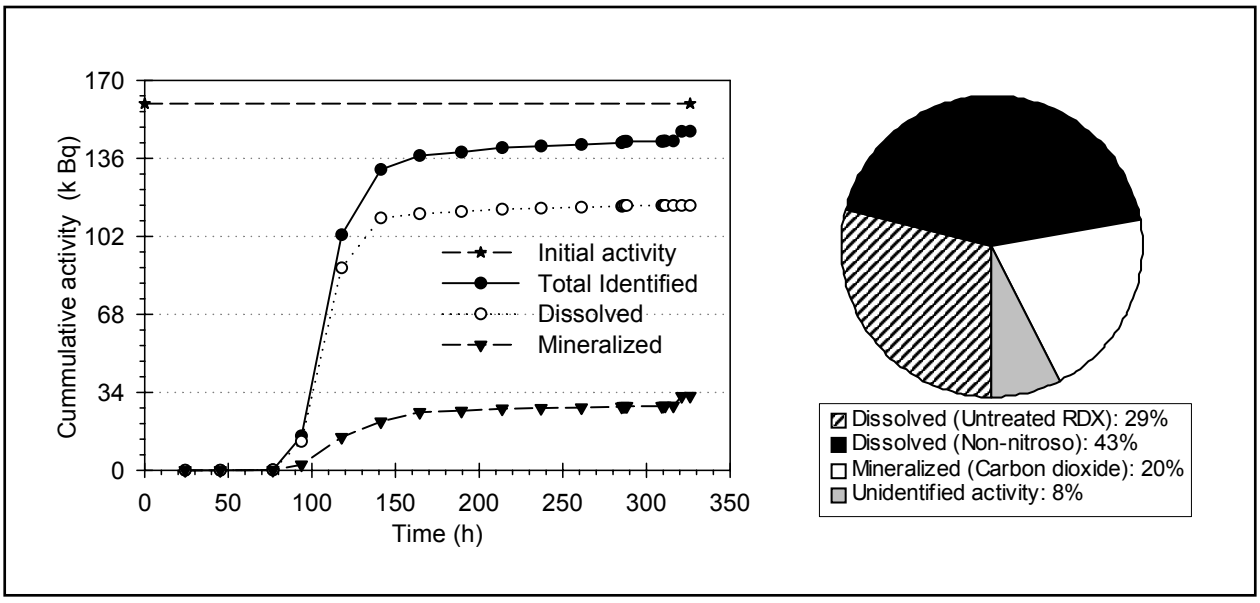

Figure 9. Distribution of ^{14}C activity from ^{14}C-RDX. The line plot shows the cumulative ^{14}C activity recovered over the test period (326 h). The time point for pie chart is the end of the radiocarbon test when no more ^{14}C activity was recovered either from the liquid or gas samples from the e^-barrier column

determined by extraction from the Carbo-Sorb. About 72 percent of the initial activity was in the dissolved phase as untreated RDX and non-nitroso derivatives. Approximately 40 percent of the total activity in the dissolved phase was unreacted ^{14}C-RDX, leaving about 60 percent of the total activity in the dissolved phase as unidentified transformation products. These products did not consist of any of the nitroso intermediates (MNX, DNX, and TNX) and are likely ring cleavage products. Additional research is required to identify these products.

The final activity balance closure indicates a failure to detect all the possible ^{14}C end products. Metabolites such as hydrazine, 1,1-dimethyl- and 1,2-dimethyl-hydrazine, methylenedinitramine (MDNA), formaldehyde, and methanol that have previously been identified (Hawari et al. 2000; McCormick et al. 1981) with reductive RDX biodegradation may have been included with the nonvolatile carbon fraction in this study. Distribution of ^{14}C over time, illustrated in Figure 9, indicates a steady increase in the identified radiocarbon fractions between 80 and 110 hr, which then stabilized over the next 130 hr without any significant increase.

TNT Transformation

The experiment using unlabeled TNT was conducted at a constant current of 20 mA (0.01 mA/cm^2) for 58 days. The resultant electric potential decreased slightly during the experiment from an initial value of approximately 15 V to approximately 12 V after 22 days. This behavior suggests that conductivity in the electrolyte increased with time and is consistent with the formation of ionic species associated with the transformation of TNT. The electrode potentials relative to the reference half-cells were constant throughout the experiment (+1.05 V SHE, -1.24 V SHE), indicating oxidation potentials less than the standard potential (+1.23 V SHE) for the oxidation of water and the reduction potential levels (reducing conditions) exceeding the standard potential (-0.80 V SHE) for the reduction of water (Figure 10). These measurements suggest that solution composition influenced the electrode potential (when compared to the RDX experiment where lower cell potential resulted in higher anode potential).

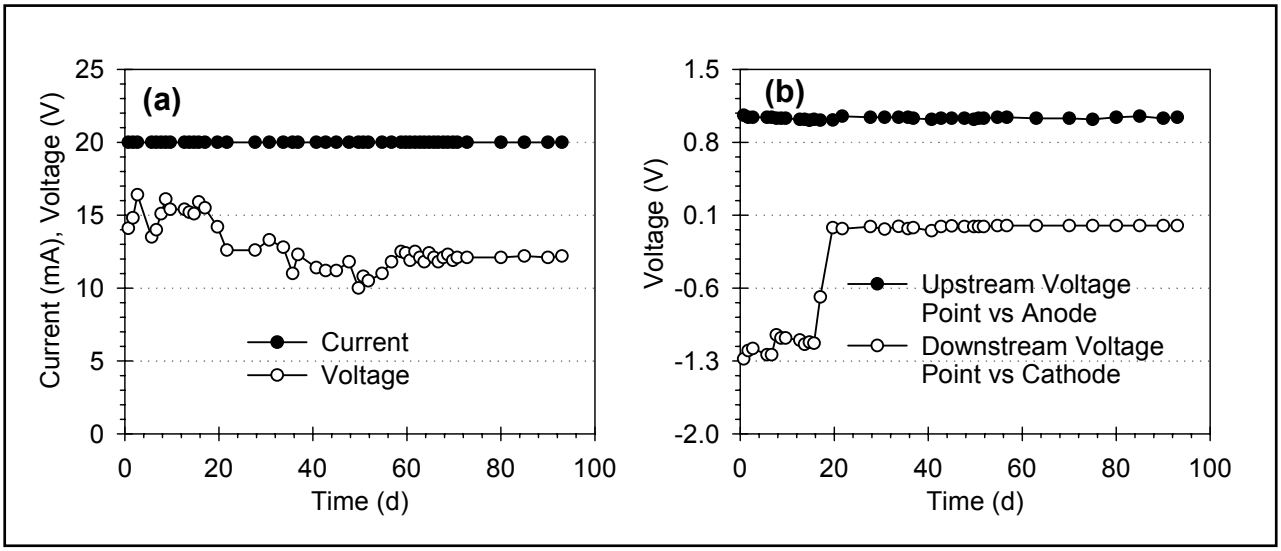

Figure 10. Operating current and voltage as a function of time for TNT test: (a) current and cell potential and (b) electrode potentials relative to Ag/AgCl reference half-cells

Influent concentrations of ~0.5 mg/L were reduced to about 0.13 mg/L without the detection of any known TNT daughter products (Figure 11). Reducing conditions were established in the column beginning with the initial time of operation. The difference in E_h between column influent (value) and effluent (value) was between 200 and 350 mV. No significant changes in aqueous pH were observed at the column inlet and outlet. However, a measurable drop in pH from 6.5 to about 3.5 was observed at the sampling port upstream of the anode, while a pH increase up to 9.5 was observed at the sampling port immediately downstream of the cathode. The high aqueous pH downstream of cathode might have partially resulted in base hydrolysis of TNT, which generally is slow at this pH (Hansen et al. 2001).

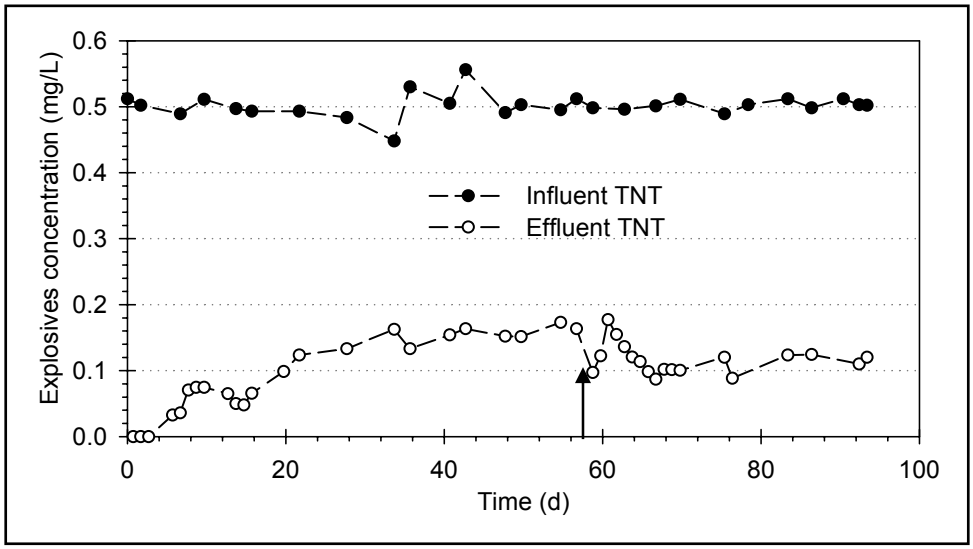

Figure 11. TNT concentration in e⁻barrier column influent and effluent stream. Arrow indicates the time when slug of radiolabel RDX was introduced

The total TNT transformation was on the order of approximately 70 percent. This unidentified 70 percent of the influent TNT concentration might have transformed to ring cleavage products in the dissolved phase or sorbed on the quartz-feldspar sand packing. The extraction of sand packing for the sorbed TNT and its transformation products was not performed for this unlabeled TNT test. Once the column reached an equilibrium state, samples from the ports along the column length were collected prior to the TNT radiocarbon study. Similar to the RDX test, TNT concentration profiles along column length demonstrated that transformation of TNT occurred primarily at the electrode set (Figure 12).

TNT Radiocarbon (^{14}C) Distribution

A slug (980.8 mL) of about 192 k Bq (~5.20 μCi) radiolabel TNT was added to the inlet reservoir on day 58, when the column was operating with steady state TNT transformation. Fifteen bed volumes of unlabeled TNT-contaminated water containing 50 percent acetone (volume basis) were pumped through the column

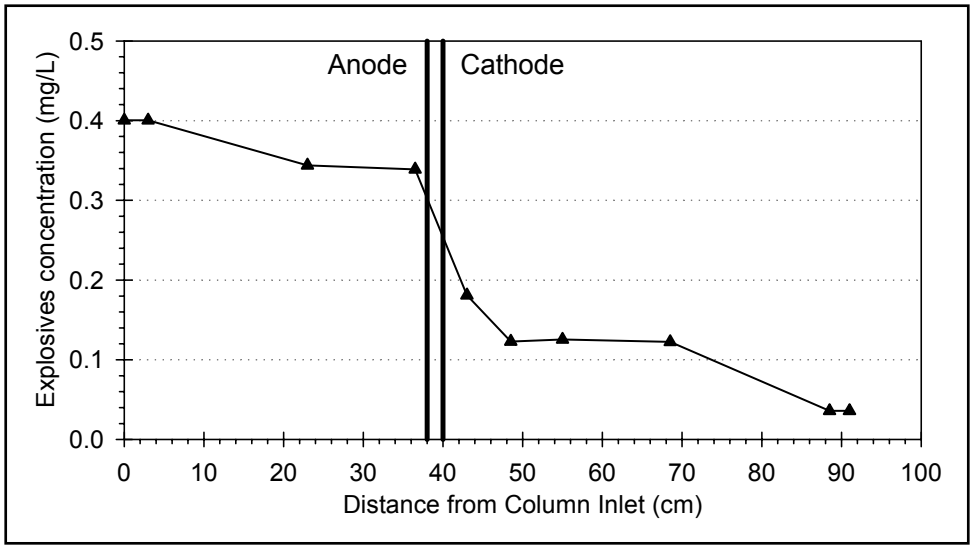

Figure 12. Axial TNT concentration profile along column length. The electrodes are set at 38 cm (anode) and 40 cm (cathode)

over the next 12 days to wash out any radioactivity sorbed on the quartz-feldspar sand pack in the column. Finally, the aliquots of the sand pack were extracted with acetonitrile, and the extractant was subject to liquid scintillation counting for estimating the sorbed fraction of radiocarbon activity. The distribution of radiocarbon (^{14}C) is summarized in Figure 13. The final activity balance on TNT radiocarbon was more than 96 percent. The radiocarbon activity was distributed into three different fractions: (a) dissolved (as aqueous soluble compounds), (b) mineralized (as carbon dioxide), and (c) sorbed (absorbed or adsorbed on the sand pack). The activity balance on ^{14}C-TNT indicated that approximately 21 percent of the influent ^{14}C activity was transformed completely to $^{14}CO_2$. Approximately 24 percent of the influent activity was sorbed to the quartz-feldspar sand pack. It is not clear if this activity is ^{14}C-TNT or a transformation product of electrolysis. Previous studies have suggested that azoxynitrotoluene polymers are formed during electrolytic transformation (Gilbert and Sale 2005) that may account for the sorbed fraction. Dissolved activity accounted for approximately 51 percent of the total initial activity, and most of it was unreacted TNT. The TNT results were similar to the RDX radiocarbon test. The distribution of ^{14}C over time (Figure 13) shows a steady increase in the identified radiocarbon fractions between 80 and 100 hr, which then stabilized over the next 120 hr without any significant increase.

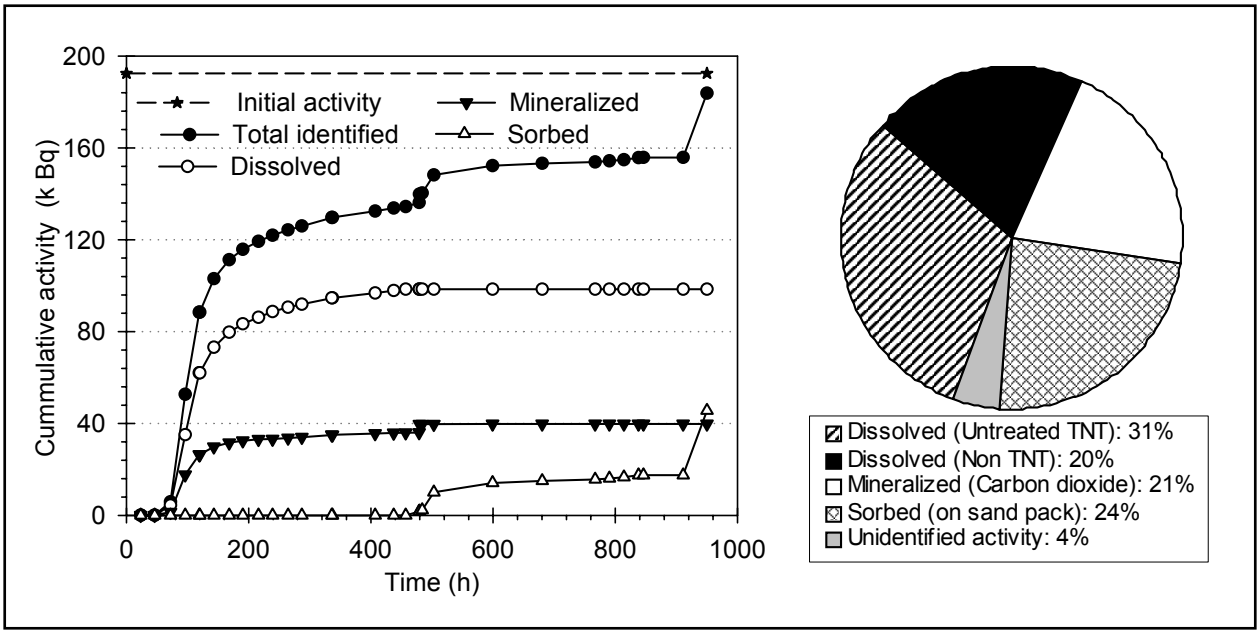

Figure 13. Distribution of ^{14}C activity from ^{14}C-TNT. The time point for pie chart is the end of the radiocarbon test when no more ^{14}C activity was recovered either from the liquid or gas samples from the column. The significant increase in the sorbed activity on the last data point represents the ^{14}C activity that was recovered from the column sand by burning the aliquots of the sand pack in Packard 307 Soil Oxidizer

4 Conclusions

This research developed an in situ electrolytic remediation technology for ORC contaminated groundwater and evaluated the mass balance of RDX and TNT electrolytic transformation in groundwater using radiolabeled RDX and TNT. A series of column studies were conducted using quartz-feldspar sand to simulate the aquifer material. The column study provides functional information on the fate of aqueous phase RDX and TNT contamination during in situ electrolytic transformation. The result of the unlabeled studies demonstrated that approximately 70 percent of influent RDX and TNT concentrations can be transformed in a single pass. No nitroso-substituted RDX transformation products or known TNT daughter products were detected in these tests. For both test contaminants (RDX and TNT), the overall activity balance closure was up to 96 percent, with about 21 percent of the initial radiocarbon mineralized to $^{14}CO_2$. However, the proportions of initial radioactivity in the dissolved fraction were different for RDX and TNT because of their different levels of sorption affinities to the column packing material. About 72 percent of the initial RDX radiocarbon was recovered as dissolved fraction, of which approximately 40 percent was unreacted ^{14}C-RDX and the remainder as non-nitroso transformation products. In the case of ^{14}C-TNT, around 51 percent of the initial activity was in the dissolved phase, with about half as untreated ^{14}C-TNT. A significant proportion (~24 percent) of ^{14}C-TNT was sorbed on the quartz-feldspar sand pack, while none of the ^{14}C-RDX was sorbed on the column packing. Although the effluent RDX concentration (150 ppb) was higher than the lifetime health advisory for RDX in drinking water (2 ppb), these results confirm the potential applicability of this type of groundwater plume control strategy and provide insight into electrolytic transformation pathways. Based on the results of this study, it is expected that in a field application more than one set of electrodes would be required to completely transform RDX and TNT to environmentally benign products.

References

Acar, Y. B., and Alshawabkeh, A. N. (1993). "Principles of electrokinetic remediation," *Environ. Sci. Technol*. 27, 2638-2647.

Alshawabkeh, A. N., and Acar, Y. B. (1992). "Removal of contaminants from soils by electrokinetics: A theoretical treatise," *J Environ. Sci. Health* A27, 1835-1861.

Balakrishnan, V. K., Halasz, A., and Hawari, J. (2003). "Alkaline hydrolysis of the cyclic nitramine explosives RDX, HMX and CL20: New insights into degradation pathways obtained by the observation of novel intermediates," *Environ. Sci. Technol*. 37, 1838-1843.

Bonin, P. M., Bejan, D., Schutt, L., Hawari, J., and Bunce, N. J. (2004). "Electrochemical reduction of hexahydro-1,3,5-trinitro-1,3,5-triazine in aqueous solutions," *Environ. Sci. Technol*. 38, 1595-1599.

Bunce, N. J., Merica, S. G., and Lipkowski, J. (1997). "Prospects for the use of electrochemical methods for the destruction of aromatic organochlorine wastes," *Chemosphere* 35, 2719-2726.

de Lima-Leite, R. H., Cognet, P., Wilhelm, A. M., and Delmas, H. (2003). "Anodic oxidation of 2,4-dihydroxybenzoic acid for wastewater treatment," *J Applied Electrochemistry* 33, 693-701.

Doppalapudi, R. B., Sorial, G. A., and Maloney, S. W. (2003). "Electrochemical reduction of 2,4-dinitrotoluene in a continuous flow laboratory scale reactor," *J Environ. Eng*. 129, 192-201.

Gilbert, D. M., and Sale, T. C. (2005). "Sequential electrolytic oxidation and reduction of aqueous phase energetic compounds," *Environ. Sci. Technol*. (Revised April 2005).

Halasz, A., Spain, J., Paquet, L., Beaulieu, C., and Hawari, J. (2002). "Insights into the formation and degradation mechanisms of methylenedinitramine during the incubation of RDX with anaerobic sludge," *Environ. Sci. Technol*. 36, 633-638.

Hansen, L. D., Ringelberg, D. D., Felt, D. R., and Davis, J. D. (2001). "Base-induced 2,4,6, trinitrotoluene transformation: Titration studies," ERDC TR-01-10, U.S. Army Engineer Research and Development Center, Vicksburg, MS.

Hawari, J., Halasz, A., Sheremata, T., Beaudet, S., Groom, C., Paquet, L., Rhofir, C., Ampleman, G., and Thiboutot, S. (2000). "Characterization of metabolites during biodegradation of hexahydro-1,3,5-trinitro-1,3,5-triazine (RDX) with municipal anaerobic sludge," *Appl. Environ. Microbiol*. 66, 2652-2657.

Jimenez-Jado, N. E., Fernandez Sanchez, C., and Ochoa Gomez, J. R. (2004). "Electrochemical degradation of nitroaromatic wastes in sulfuric acid solutions: Part 1," *J Applied Electrochemistry* 34, 551-556.

Jolas, J. L., Pehkonen, S. O., and Maloney, S. W. (2000). "Reduction of 2,4-dintitrotoluene with graphite and titanium mesh cathodes," *Water Environ. Res*. 72, 179-188.

Maloney, S. W., Pehkonen, S., Jolas, J. L., and Meenakshisundaram D. (1999) "Electrochemical reduction of dinitrotoluene," Report Number 99/89, ADA Number 372795, Coastal Engineering Research Laboratory, U.S. Army Engineer Research and Development Center, Champaign, IL.

McCormick, N. G., Cornell, J. H., and Kaplan, A. M. (1981). "Biodegradation of hexahydro-1,3,5-trinitro-1,3,5-triazine," *Appl. Environ. Microbiol*. 42, 817-823.

Mills, A., Seth, A., and Peters, G. (2003). "Alkaline hydrolysis of trinitrotoluene, TNT," *Phys. Chem. Chem. Phys*. 5, 3921-3927.

Oh, B-T., Just, C. L., and Alvarez, P. J .J. (2001). "Hexahydro-1,3,5-trinitro-1,3,5-triazine mineralization by zerovalent iron and mixed anaerobic cultures," *Environ. Sci. Technol*. 35, 4341-4346.

Panizza, M., and Cerisola, G. (2004). "Influence of anode material on the electrochemical oxidation of 2-napthol - Part 2. Bulk electrolysis experiments," *Electrochemical Acta* 49, 3221-3226.

Probstein, R. F., and Hicks, R. E. (1993). "Removal of contaminants from soils by electric fields," *Science* 260, 498-504.

Rodgers, J. D., and Bunce, N. J. (2001). "Electrochemical treatment of 2,4,6-trinitrotoluene and related compounds," *Environ. Sci. Technol*. 35, 406-410.

Roessler, A., Crettenand, D., Dossenbach, O., Marte, W., and Rys, P. (2002). "Direct electrochemical reduction of indigo," *Electrochemical Acta* 47, 1989-1995.

Sale, T. C., Gilbert, D. M., and Petersen, M. A. (2005). "Cost and performance report: Electrically induced redox barriers for treatment of groundwater." ESTCP Project CU0112.

Vlyssides, A. G., Karlis, P. K., and Mahnken, G. (2003). “Influence of various parameters on the electrochemical treatment of landfill leach,” *J Appl. Electrochem*. 33, 155-159.

Appendix A
Column Hydrodynamics

A tracer test was performed to evaluate the hydrodynamic properties of the quartz-feldspar sand pack in the column. The tracer test was performed by adding chloride at a nontoxic level and sampling the effluent periodically to develop a breakthrough curve. The measured hydraulic retention time with the chloride concentration analysis data were used in the advection-dispersion model to determine dispersivity and the bed porosity:

$$\frac{\partial C}{\partial t} = \alpha v \frac{\partial^2 C}{\partial x^2} - v \frac{\partial C}{\partial x} \qquad \text{(A1)}$$

where

C = chloride concentration (mg/L)

t = time elapsed (hr)

α = dispersivity (cm)

v = $q/(A*n)$, average interstitial or pore water velocity (cm/hr)

q = groundwater flow (mL/hr)

A = column cross-section area (cm^2)

n = aquifer material porosity

x = distance from the column inlet (cm)

Given the initial condition $C(x,0) = 0$ and boundary conditions $C(0,t) = C_0$ and $\partial C/\partial x(\infty,t) = 0$, the solution to Equation A1 is shown in Equation A2:

$$C = \frac{C_O}{2}\left[erfc\left(\frac{x - vt}{2\sqrt{\alpha v t}}\right) + \exp\left(\frac{x}{\alpha}\right) erfc\left(\frac{x + vt}{2\sqrt{\alpha v t}}\right)\right] \qquad \text{(A2)}$$

REPORT DOCUMENTATION PAGE

Form Approved
OMB No. 0704-0188

1. REPORT DATE *(DD-MM-YYYY)*	2. REPORT TYPE	3. DATES COVERED *(From - To)*
August 2005	Final report	

4. TITLE AND SUBTITLE

Electrolytic Transformation of Hexahydro-1,3,5-Trinitro-1,3,5-Triazine (RDX) and 2,4,6-Trinitrotoluene (TNT) in Aqueous Solutions

5a. CONTRACT NUMBER

5b. GRANT NUMBER

5c. PROGRAM ELEMENT NUMBER

6. AUTHOR(S)

Altaf H. Wani, Brenda R. O'Neal, David M. Gilbert, David B. Gent, Jeffrey L. Davis

5d. PROJECT NUMBER

5e. TASK NUMBER

5f. WORK UNIT NUMBER
EQT D03E

7. PERFORMING ORGANIZATION NAME(S) AND ADDRESS(ES)

See reverse.

8. PERFORMING ORGANIZATION REPORT NUMBER

ERDC/EL TR-05-10

9. SPONSORING / MONITORING AGENCY NAME(S) AND ADDRESS(ES)

U.S. Army Corps of Engineers
Washington, DC 20314-1000

10. SPONSOR/MONITOR'S ACRONYM(S)

11. SPONSOR/MONITOR'S REPORT NUMBER(S)

12. DISTRIBUTION / AVAILABILITY STATEMENT

Approved for public release; distribution is unlimited.

13. SUPPLEMENTARY NOTES

14. ABSTRACT

Electrolytic reactive barriers (e⁻barriers) consist of closely spaced permeable electrodes installed across a groundwater contaminant plume in a permeable reactive barrier format. Application of sufficient potential to the electrodes results in sequential oxidation and reduction of the target contaminant. The objective of this study was to quantify the mass distribution of compounds produced during sequential electrolytic oxidation and reduction of ordinance related compounds (ORCs) in a laboratory analog to an e⁻barrier. In this study, a series of column tests were conducted using RDX (hexahydro-1,3,5-trinitro-1,3,5-triazine) and TNT (2,4,6-trinitrotoluene) as representative ORCs. The experimental setup consisted of a Plexiglass column packed with quart-feldspar sand to simulate aquifer conditions. A single set of porous electrodes consisting of expanded titanium-mixed metal oxide mesh was placed at the midpoint of the soil column as a one-dimensional analog to an e⁻barrier. Constant current of 20 mA (variable voltage) was applied to the electrode set. Initial studies involved quantification of reaction products using unlabeled RDX and TNT. Approximately 70 percent of the influent concentration was transformed, in one pass, through sequential oxidation-reduction for both contaminants. Following the unlabeled studies, ^{14}C labeled RDX and TNT were introduced to determine the mass balance. An activity balance of up to 96 percent was

(Continued)

15. SUBJECT TERMS

e⁻barrier	^{14}C-TNT	In situ electrolytic transformation
^{14}C-RDX	Groundwater	Ordnance related compounds

16. SECURITY CLASSIFICATION OF:			17. LIMITATION OF ABSTRACT	18. NUMBER OF PAGES	19a. NAME OF RESPONSIBLE PERSON
a. REPORT	b. ABSTRACT	c. THIS PAGE			19b. TELEPHONE NUMBER *(include area code)*
UNCLASSIFIED	UNCLASSIFIED	UNCLASSIFIED	SAR	28	

7. (Concluded)

Applied Research Associates, Inc.
Southern Division
119 Monument Place
Vicksburg, MS 39180-6199;

Analytical Services, Inc.
3532 Manor Drive
Vicksburg, MS 39180-6199;

Department of Civil Engineering
Colorado State University
Fort Collins, CO 80523;

Environmental Laboratory
U.S. Army Engineer Research and Development Center
3909 Halls Ferry Road
Vicksburg, MS 39180-6199

14. (Concluded)

achieved for both ^{14}C-RDX and ^{14}C-TNT. For both contaminants, approximately 21 percent of the influent activity was mineralized to $^{14}CO_2$. The proportion of the initial activity in the dissolved fraction was different for the two test contaminants. Approximately 30 percent of the initial ^{14}C-RDX was recovered as unreacted in the dissolved phase. The balance of the ^{14}C-RDX was recovered as non-volatile, non-nitroso transformation products. None of the ^{14}C-RDX was sorbed to the column sand packing. For ^{14}C-TNT approximately 51 percent of the initial activity was recovered in the dissolved phase, the majority being unreacted TNT. The balance of the ^{14}C-TNT was either sorbed to the sand packing (approximately 24 percent) or dissolved/mineralized as unidentified ring cleavage products (~4 percent).